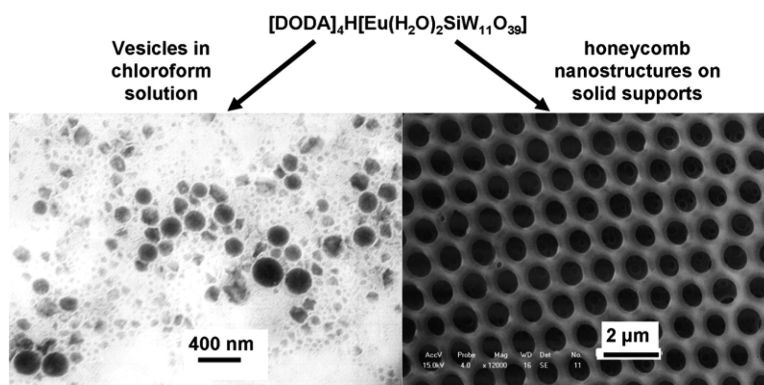


## Polyoxometalate-Based Vesicle and Its Honeycomb Architectures on Solid Surfaces

Weifeng Bu, Haolong Li, Hang Sun, Shengyan Yin, and Lixin Wu

*J. Am. Chem. Soc.*, **2005**, 127 (22), 8016-8017 • DOI: 10.1021/ja042980j • Publication Date (Web): 12 May 2005

Downloaded from <http://pubs.acs.org> on March 25, 2009



### More About This Article

Additional resources and features associated with this article are available within the HTML version:

- Supporting Information
- Links to the 13 articles that cite this article, as of the time of this article download
- Access to high resolution figures
- Links to articles and content related to this article
- Copyright permission to reproduce figures and/or text from this article

[View the Full Text HTML](#)

## Polyoxometalate-Based Vesicle and Its Honeycomb Architectures on Solid Surfaces

Weifeng Bu, Haolong Li, Hang Sun, Shengyan Yin, and Lixin Wu\*

Key Laboratory for Supramolecular Structure and Materials of Ministry of Education, Jilin University, Changchun 130012, People's Republic of China

Received November 21, 2004; E-mail: wulx@jlu.edu.cn

Polyoxometalates (POMs) are intriguing nanosized inorganic clusters due to their structural, chemical, and electronic versatility, and thus potential application as materials for catalysis, energy storage, biomedicine, and surface coatings.<sup>1</sup> Combined with molecular membrane chemistry, the metal–oxide clusters can be manipulated efficiently through cooperative electrostatic interactions, forming multifunctional organic/inorganic materials. Cationic surfactants can replace the counterions of POMs and modify their surface chemistry properties, yielding surfactant-encapsulated clusters (SECs).<sup>2,3</sup> Encapsulation by cationic surfactants not only increases solubility of POMs in organic media, thus facilitating mesoscopic supramolecular assembly of POMs,<sup>2,3</sup> but also exerts a remarkable influence on POMs' electronic properties.<sup>3d,g</sup> Well-ordered thin films of SECs are readily prepared by Langmuir–Blodgett and solvent-casting methods. We wonder if we could generate technologically useful architectures on solid substrates based on these supramolecular soft materials through a stepwise self-assembled process, although a soft lithographic approach has been demonstrated for the fabrication of two-dimensional micro-sized patterns of SECs.<sup>4</sup>

Infinite one-dimensional POMs have been synthesized based on lanthanide and monolacunary Keggin [SiW<sub>11</sub>O<sub>39</sub>]<sup>8-</sup> with a stoichiometric ratio of 1:1.<sup>5</sup> These one-dimensional structures exist in crystalline states linked by the weak Ln–O<sub>d</sub> bonds; they are easily disrupted and dissociated into monomeric building blocks in aqueous solution. The luminescence decay lifetime of the <sup>5</sup>D<sub>0</sub> state of [Eu(H<sub>2</sub>O)<sub>2</sub>SiW<sub>11</sub>O<sub>39</sub>]<sup>5-</sup> (POM-1, 0.37 ms) is a diagnostic signal for the transition from chain structure to monomeric entity [Eu(H<sub>2</sub>O)<sub>4</sub>SiW<sub>11</sub>O<sub>39</sub>]<sup>5-</sup> (0.205 ms)<sup>5b</sup> in aqueous phase. Here, we find when POM-1 is encapsulated with dimethyl dioctadecylammonium (DODA), it forms a supramolecular complex of (DODA)<sub>4</sub>H-[Eu(H<sub>2</sub>O)<sub>2</sub>SiW<sub>11</sub>O<sub>39</sub>] (SEC-1), which aggregates into vesicles in chloroform solution, and when cast onto solid supports, forms honeycomb structures. This technique would allow us to fabricate advanced nanodevices exhibiting the multifunctional properties of POMs.

SEC-1 exhibits the characteristic <sup>5</sup>D<sub>0</sub> → <sup>7</sup>F<sub>*j*</sub> (*j* = 0, 1, 2, 3, 4) Eu<sup>3+</sup> emissions. The fluorescent lifetimes of SEC-1 in the solid state and chloroform solution (Figure 1A and B) are 0.42 and 0.52 ms, respectively, with a single-exponential decay, similar to that of the chainlike POM-1 in the solid state, but much larger than that of the monomeric POM-1 in aqueous solution (vide supra).<sup>5b</sup> Replacement of the OH oscillators by OD makes the vibronic de-excitation pathway exceedingly inefficient.<sup>6</sup> Therefore, the number of water molecules coordinated to Eu<sup>3+</sup> (*q*) can be calculated with an estimated uncertainty of 0.5, according to the following equation:  $q = 1.05(1/\tau_{H_2O} - 1/\tau_{D_2O})$  (1), where  $\tau_{H_2O}$  and  $\tau_{D_2O}$  are the experimental excited-state lifetimes (ms) in H<sub>2</sub>O and D<sub>2</sub>O, respectively.<sup>6</sup> The number of water molecules coordinated to Eu<sup>3+</sup> in the solid state and chloroform solution of SEC-1 is calculated

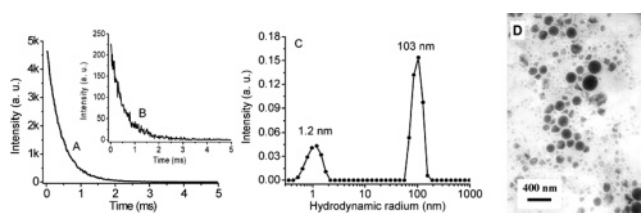


**Figure 1.** Luminescence decay curves of SEC-1 at its solid state (A), chloroform solution (B), DLS CONTIN plots of the  $R_h$  of SEC-1 in chloroform solution (1 mg/mL) (C), and TEM image (D).

to be 1.5 and 1.1, respectively, within the range of elemental analysis accuracy. These data suggest that the temporary or permanent weak Eu–O<sub>d</sub> linkers appear between adjacent POM-1 clusters, which would imply supramolecular aggregates in both the solid and solution of SEC-1. Small-angle X-ray scattering (SAXS) measurement in the chloroform solution of SEC-1 shows the presence of large nanosized aggregates (20–32 nm, centered at 25 nm) as obtained from the distance distribution function. Considering the size limits, thus accuracy of the SAXS measurement,<sup>7a</sup> SEC-1 solution is further characterized by dynamic light scattering (DLS), which will provide the hydrodynamic radius,  $R_h$ , of this organic/inorganic hybrid. As shown in the CONTIN plot in Figure 1C, two modes exist. The small peak has an average  $R_h$  of 1.2 nm, corresponding to the monomeric SEC-1. The second peak has a narrow size distribution, and the  $R_h$  is about 103 nm, suggesting the formation of a uniform aggregate in the chloroform solution. Transmission electron microscopy (TEM) studies confirm the supramolecular aggregates are vesicles of SEC-1 in the chloroform solution (Figure 1D), and size range of the vesicles is consistent with the DLS measurement. POM-based vesicles have been observed in the polyoxomolybdate solution before.<sup>7</sup> Our results here suggest that POM-based vesicles also exist in the surfactant-encapsulated heteropolyoxotungstate systems, and their sizes are larger than those in the polyoxomolybdate-based solution ( $R_h$  = 34–45 nm). <sup>183</sup>W and <sup>29</sup>Si NMR measurements of SEC-1 in CDCl<sub>3</sub> failed, which is not surprising given the fact that SEC-1 has a very large  $R_h$  (60–150 nm), consequently a lower mobility of POM-1. X-ray diffraction (XRD) of solid SEC-1 reveals that SEC-1 possesses a lamellar structure with a spacing of 4.5 nm and the lateral packing of DODA alkyl chains at 0.42 nm. Combining the lamellar distance of DODA (3.811 nm)<sup>8</sup> and the radius of the monomeric POM-1 (0.52 nm),<sup>5b</sup> we infer that the fitting spacing of SEC-1 should be 4.8 nm, which agrees well with the experimental value. This lamellar organized material is reminiscent of those polyelectrolyte–surfactant complexes (PSCs),<sup>9</sup> in which POM-1 layers are alternated with the DODA bilayer.

Solvent-casting film of SEC-1 is prepared from chloroform solution (2 mM) under a moist airflow across the solution surface. The films exhibit bright iridescent colors when viewed with reflected light, indicating a periodic refractive index of variation

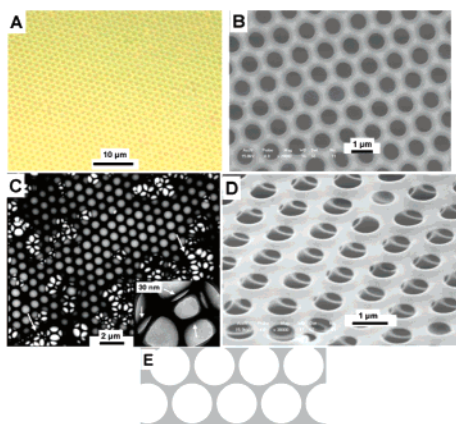


**Figure 2.** The honeycomb-structured film of SEC-1: (A) optical micrograph, (B) SEM, (C) TEM images, and (D) SEM image obtained from the sample against an electron beam at an angle of 50°. (E) Schematic cross-section of this regular microporous film.

through the film thickness.<sup>10a,b</sup> Optical micrograph reveals a regular hexagonal array of spherical cavities (Figure 2A) covering a wide area. Scanning electron microscopy (SEM) image (Figure 2B) confirms this observation and shows that the surface holes have a regular size of about 800 nm with an interspacing around 600 nm. TEM shows that the film is composed of multilayers of empty spheres (Figure 2C, arrow). Besides this honeycomb pattern, the magnified TEM image (Figure 2C Inset) shows the presence of linear aggregates with a width of 20–40 nm in the void, which is in good agreement with the scanning force microscopy (SFM) data of a spin-coating film of SEC-1. The width is much larger than that of the lamellar distance (4.5 nm) of SEC-1 obtained from its XRD. Therefore, they should be higher order aggregates of SEC-1. The internal honeycomb architectures are further observed by SEM, in which the sample was oriented against an electron beam at an angle of 50° (Figure 2D). The internal thickness of the microporous wall is about 100 nm, and the diameter of the internal holes is around 1.3  $\mu\text{m}$ . A schematic cross-section of this regular microporous film is shown in Figure 2E. To the best of our knowledge, this is the first example of POM-based microsized stereoarchitecture prepared by stepwise self-assembly. Generally, the honeycomb architectures are formed at a relative humidity of >50%.<sup>10c</sup> The honeycomb structure of SEC-1 could not be obtained by evaporation of the chloroform solution under a relatively dry atmosphere (relative humidity < 30%). SFM image shows nanosheets and nanowires in those casting films. The different surface morphology of the two kinds of casting films mentioned above leads to their different surface wettability. The water contact angle of the casting film prepared under relatively dry atmosphere is 110°, whereas the honeycomb-architected film offers a contact angle of 132°. Interestingly, X-ray diffraction shows that both of the casting films have a lamellar structure with a spacing of 3.6 nm. Compared to those of the solid-state SEC-1, the alkyl chains in the casting films are proposed to possess a partial interdigitation with an interdigitated length of 0.9 nm. Therefore, SEC-1 is reorganized from vesicles in the chloroform solution into a DODA bilayer structure alternated with POM-1 layers at the air/solid interface, which is similar to the synthetic bilayer membranes.<sup>11</sup>

The observed honeycomb pattern and the condition under which it is prepared are reminiscent of the microporous films formed by the solvent evaporation of copolymers, star-shaped polymers, and PSCs.<sup>10</sup> In these micro/nanophase separation systems, the rapid solvent evaporation decreases the air–solution interfacial temperature below the dew point of water, leading to a hexagonal array of condensed micrometer-sized water droplets of the moisture on

the casting films. This regular array acts as a template to direct the formation of the honeycomb architectures. In our case, nanophase separation happens between the incompatible POM-1 and DODA side chains, which are linked by electrostatic interactions, similar to that of PSCs.<sup>9</sup> Here, a similar mechanism for the formation of this highly ordered microporous structure is proposed.

In summary, the introduction of cationic surfactant DODA as counterions of  $[\text{Eu}(\text{H}_2\text{O})_2\text{SiW}_{11}\text{O}_{39}]^{5-}$  forms an organic/inorganic hybrid mesoscopic supramolecular assembly of  $(\text{DODA})_4\text{H}[\text{Eu}(\text{H}_2\text{O})_2\text{SiW}_{11}\text{O}_{39}]$ , which aggregates into vesicles in chloroform solution. The POM-based vesicles can be transferred into three-dimensional ordered arrays that range from micrometric sizes. The POM-based vesicle and honeycomb architecture would create opportunities for the development of new materials for semiconducting devices and separation membranes. The present methodology suggests that combining inorganic chemistry and colloidal surface chemistry may allow us to generate technology-applicable microsized patterns of inorganic functional units, through stepwise self-assembly of preorganized building blocks, that is, supramolecular synthons, which would provide an alternative for the soft lithographic method.<sup>12</sup>

**Acknowledgment.** The authors acknowledge the financial support from the National Natural Science Foundation of China (Grant No. 20473032), the Major State Basic Research Development Program (Grant No. G2000078102), the PCSIRT of Ministry of Education of China, and the Innovation Fund of Jilin University.

**Supporting Information Available:** The characterization for SEC-1, <sup>1</sup>H NMR, XRD, fluorescent spectra, SFM images, SAXS, and soft lithography patterns of SECs. This material is available free of charge via Internet at <http://pub.acs.org>.

## References

- (1) (a) Pope, M. T.; Müller, A. *Angew. Chem., Int. Ed.* **1991**, *30*, 34–48. (b) Hill, C. L.; Prosser-McCarthy, C. M. *Coord. Chem. Rev.* **1995**, *143*, 407–455. (c) Hill, C. L. *Chem. Rev.* **1998**, *98*, 1–390 (the entire issue is devoted to polyoxometalates). (d) Casañ-Pastor, N.; Gómez-Romero, P. *Front. Biosci.* **2004**, *9*, 1759–1770.
- (2) (a) Kurth, D. G.; Lehmann, P.; Volkmer, D.; Cölfen, H.; Koop, M. J.; Müller, A.; Du Chesne, A. *Chem.—Eur. J.* **2000**, *6*, 385–393. (b) Volkmer, D.; Du Chesne, A.; Kurth, D. G.; Schnablegger, H.; Lehmann, P.; Koop, M. J.; Müller, A. *J. Am. Chem. Soc.* **2000**, *122*, 1995–1999. (c) Kurth, D. G.; Lehmann, P.; Volkmer, D.; Müller, A.; Schwahn, D. *J. Chem. Soc., Dalton Trans.* **2000**, 3989–3998.
- (3) (a) Bu, W.; Wu, L.; Hou, X.; Fan, H.; Hu, C.; Zhang, X. *J. Colloid Interface Sci.* **2002**, *251*, 120–124. (b) Bu, W.; Fan, H.; Wu, L.; Hou, X.; Hu, C.; Zhang, G.; Zhang, X. *Langmuir* **2002**, *18*, 6398–6403. (c) Bu, W.; Zhang, J.; Wu, L.; Tang, A.-C. *Chin. J. Chem.* **2002**, *20*, 1514–1458. (d) Bu, W.; Wu, L.; Zhang, X.; Tang, A.-C. *J. Phys. Chem. B* **2003**, *107*, 13425–13431. (e) Bu, W.; Wu, L.; Tang, A.-C. *J. Colloid Interface Sci.* **2004**, *269*, 472–475. (f) Bu, W.; Li, W.; Li, H.; Wu, L.; Tang, A.-C. *J. Colloid Interface Sci.* **2004**, *274*, 200–203. (g) Bu, W.; Li, H.; Li, W.; Wu, L.; Zhai, C.; Wu, Y. *J. Phys. Chem. B* **2004**, *108*, 12776–12782.
- (4) Bu, W.; Wu, L. Unpublished results (Supporting Information, Figure S6).
- (5) (a) Sadakane, M.; Dickman, M. H.; Pope, M. T. *Angew. Chem., Int. Ed.* **2000**, *39*, 2914–2916. (b) Mialane, P.; Lissard, L.; Mallard, A.; Marrot, J.; Antic-Fidancev, E.; Aschehoug, P.; Vivien, D.; Sécheresse, F. *Inorg. Chem.* **2003**, *42*, 2102–2108.
- (6) Horrocks, W. D., Jr.; Sudnick, D. R. *Acc. Chem. Res.* **1981**, *14*, 384–392.
- (7) (a) Müller, A.; Diemann, E.; Kuhlmann, C.; Eimer, W.; Serain, C.; Tak, T.; Knechel, A.; Pranzas, P. K. *Chem. Commun.* **2001**, 1928–1929. (b) Liu, T. *J. Am. Chem. Soc.* **2002**, *124*, 10942–10943. (c) Liu, T.; Diemann, E.; Li, H.; Dress, A. W. M.; Müller, A. *Nature* **2003**, *426*, 59–62. (d) Liu, T. *J. Am. Chem. Soc.* **2003**, *125*, 312–313. (e) Liu, T. *J. Clust. Sci.* **2003**, *14*, 215–226.
- (8) Okuyama, K.; Soboi, Y.; Iijima, N.; Hirabayashi, K.; Kunitake, T.; Kajiyama, T. *Bull. Chem. Soc. Jpn.* **1988**, *61*, 1485–1490.
- (9) (a) Ober, C. K.; Wegner, G. *Adv. Mater.* **1997**, *9*, 17–31. (b) Thünemann, A. F. *Prog. Polym. Sci.* **2002**, *27*, 1473–1572.
- (10) (a) Widawski, G.; Rawiso, M.; Francois, B. *Nature* **1994**, *369*, 387–389. (b) Srinivasarao, M.; Collings, D.; Philips, A.; Patel, S. *Science* **2001**, *292*, 79–83. (c) Karthaus, O.; Maruyama, N.; Cieren, X.; Shimomura, M.; Hasegawa, H.; Hashimoto, T. *Langmuir* **2000**, *16*, 6071–6076.
- (11) Kunitake, T. *Angew. Chem., Int. Ed.* **1992**, *31*, 709–726.
- (12) Xia, Y.; Whitesides, G. M. *Angew. Chem., Int. Ed.* **1998**, *37*, 550–575.

JA042980J